This paper must be cited as:

VNIVERSITAT DØ VALÈNCIA

The final publication is available at

On the Performance of a Linearized Dual Parallel Mach-Zehnder Electro-Optic Modulator

J. Perez[1] and R. Llorente[2]

[1] Optical Communications Research Group, Faculty of Engineering and Environment,Northumbria University, Newcastle-upon-Tyne, NE1 8ST, UK.

[2] Nanophotonics Technology Center, Universitat Politècnica de València, C/ Camino de Vera s/n, Valencia 46022 Spain.

E-mail: joaquin.perez@northumbria.ac.uk

Fax: +44 (0)191 243 7630

Abstract—The performance of a dual parallel differential Mach-Zehnder modulator broadband linearization architecture is analysed. This study provides experimental and analytical results showing an enhancement up to 20 dB in the 3rd-order intermodulation distortion factor at 5 GHz using RF and optical asymmetrical feeding factors.

Keywords— optical fibre communications, fibre radio, modulator, linearisation techniques, microwave photonics

1. Introduction

Over the last decade, a number of bandwidth hungry applications and services have appeared, e.g., HD streaming, mobile broadband and online gaming. To address this high bandwidth demand, ubiquitous and high data-rate access technologies have emerged based on a range of wireless, fibre and optical-wireless technologies, e.g. radio-over-fibre (RoF). However, RoF systems performance, e.g. dynamic range, is limited by the nonlinear response of the optical transmitters, e.g. electro-optical modulator (EOM). EOM exhibit an inherent non-linear behaviour, which is reflected in a non-linear transfer function due to different factors, e.g., bias wavelength and polarization dependence or environmental factors [1]. Therefore, this non-linear behaviour limits the EOM dynamic range (DR) and degrades modulation performance, improving the presence of intermodulation distortion (IMD) in analog applications where EOM is a key element, such as wide-band analog fibre optic links.

Several techniques have been proposed to linearize the EOM transfer function using pre-distortion and post-distortion electronic circuit. For example, performing a dynamic bias control [2] or designing an appropriate electrode to decrease wavelength EOM dependence [3], which limits the EOM optical bandwidth. On the other hand, optical linearization techniques [1], based on parallel and serial Mach-Zehnder modulator (MZM) architectures achieve broadband EOM linearization [4-7].

2. Linearization technique

The aim of this letter is to analyse an optical broadband linearization technique, based on the dual parallel differential MZM (DPD-MZM) architecture shown in Figure 1. A similar dual MZM structure has been proposed previously in [5, 6] and recently on a single-drive dual-parallel MZM [7, 8]. The proposed DPD-MZM architecture considers two parallel MZM with asymmetric optical signal (α) and electrical radiofrequency (RF) signal (β) feeding. A parallel MZM architecture [9] compared with a single MZM achieves an improvement of 10 dB spurious-free dynamic range (SFDR), as shown in [3]. In the proposed scheme, the use of opposite quadrature bias point (QB) and optical and electrical asymmetric feeding in the

DPD-MZM architecture results in a significant increase of the SFDR as it is stated in this paper, as SFDR is an important quality factor in analog systems [10]. The proposed linearization technique is based on the asymmetric electrical and optical feeding of each MZM in a dual parallel architecture. This technique performs a maximum optical power in one branch and minimum on the toher thanks to the factor alpha, as depicted in Figure 1.If in one MZM branch of the DPD-MZM the optical power is maximum (alpha factor) then the electrical RF signal is the lower value due to the inverse asymmetric electrical feeding factor beta. This inverse and asymmetrical behaviour allow to minimize the fifth order intermodulation harmonic components in the MZM branch with lower electrical RF signal and minimize the RF power of the third order intermodulation harmonic components on the other MZM branch with low optical signal. After the photodetection a linearized RF signal with improved rejection to the third order intermodulation harmonics will arise, as proposed in Figure 1. Moreover, the proposed DPD-MZM scheme can be used to any multioctave optical link to obtain a high dynamic-range system.
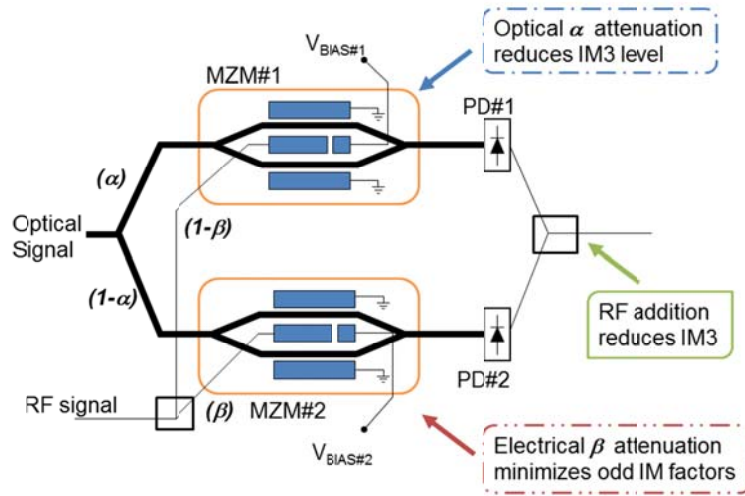

Figure 4. Proposed DPD-MZM internal architecture, where PD#i is photodetector i.

Let us first analyse a single MZM. In this case, the power transfer function is given by:

$$P_{out} = P_{in} \cdot L_{ff} \left(\left(1 + \cos\left(\frac{\pi}{V_{pi}} \left(V_1 - V_2 \right) \right) \right) \right) , \tag{1}$$

where L_{ff} includes modulator losses, and $\frac{\pi}{V_{pi}}\left(V_1 - V_2 \right) \propto m_{DC} + m_1 \sin\left(\omega_1 t + \phi_1 \right) + m_2 \sin\left(\omega_2 t + \phi_2 \right)$ with

$m_i = V_i/V_{pi}$ modulation index, and ϕ_i and ω_i re the phase and frequency of the RF signal on each modulator, respectively.

The expression (1) can be rewritten in terms of Bessel functions [11] as follows:

$$P_{out} = P_{in} \cdot L_{ff} \cdot \begin{pmatrix} 1+\cos(m_{DC}) \begin{pmatrix} \sum_{j=-\infty}^{\infty}\sum_{k=-\infty}^{\infty} J_{2j}(m_1)J_{2k}(m_2)\cos(2j\omega_1 t + 2k\omega_2 t) + \\ +\sum_{j=-\infty}^{\infty}\sum_{k=-\infty}^{\infty} J_{2j+1}(m_1)J_{2k+1}(m_2)\cos\big((2j+1)\omega_1 t + (2k+1)\omega_2 t\big) \end{pmatrix} + \\ +\sin(m_{DC}) \begin{pmatrix} \sum_{j=-\infty}^{\infty}\sum_{k=-\infty}^{\infty} J_{2j+1}(m_1)J_{2k}(m_2)\sin\big((2j+1)\omega_1 t + 2k\omega_2 t\big) + \\ +\sum_{j=-\infty}^{\infty}\sum_{k=-\infty}^{\infty} J_{2j}(m_1)J_{2k+1}(m_2)\cos\big(2j\omega_1 t + (2k+1)\omega_2 t\big) \end{pmatrix} \end{pmatrix}. \qquad (2)$$

From the above expression, non-linear distortion IMD terms related to third order intermodulation distortion (IM$_3$) and third harmonic order (HD$_3$), can be easily identified. When the single MZM is biased at $m_{DC} = \pi/2$ or QB, only odd non-linear terms are included in equation (2).

Let us now evaluate the dependence of (2) with the asymmetric feeding factors at the proposed dual DP-MZM scheme. Given two parallel MZM biased at QB, and assuming that the optical signal is photodetected by an ideal photodetector with responsivity, $\Re$, equations (3) and (4) reflect 1st- and 3rd-order terms present in the photodetected current signal of dual PD-MZM:

$$i_{out}(\omega_1) = P_{opt}\Re L_{ff}\begin{bmatrix} -\alpha J_1(\beta m)J_0(\beta m) + \\ +(1-\alpha)J_1((1-\beta)m)J_0((1-\beta)m) \end{bmatrix}, \qquad (3)$$

$$i_{out}(2\omega_1-\omega_2) = P_{opt}\Re L_{ff}\begin{bmatrix} \alpha J_2(\beta m)J_1(\beta m) + \\ +(1-\alpha)J_2((1-\beta)m)J_1((1-\beta)m) \end{bmatrix}, \qquad (4)$$

where; $\{\alpha,\beta\} \in [0,1]$. Therefore, the main 3rd-order distortion factors can be expressed as:

$$\begin{aligned} IM_3 &= i_{out}(\omega_1)/i_{out}(2\omega_1-\omega_2) \\ HD_3 &= i_{out}(\omega_1)/i_{out}(\omega_3) \end{aligned}. \qquad (5)$$

Simulations have been performed to determine α and β factors that maximize IM_3 and HD_3 factors under ideal conditions, based on expressions (3)-(5). The IM_3 and carrier (H_0) simulated results are show in Figure 2.

In Figure 2 it can be observed than selecting a 15% electrical feeding and 65% optical feeding factors provides rejection of nearly 60 dB IM_3 with a 60 dB H_0. Moreover, considering other pair of α and β feeding factors to achieve maximum IM_3 value would decrease H_0 power. That constraint has to be considered in order to analyse and implement a real DPD-MZM architecture.
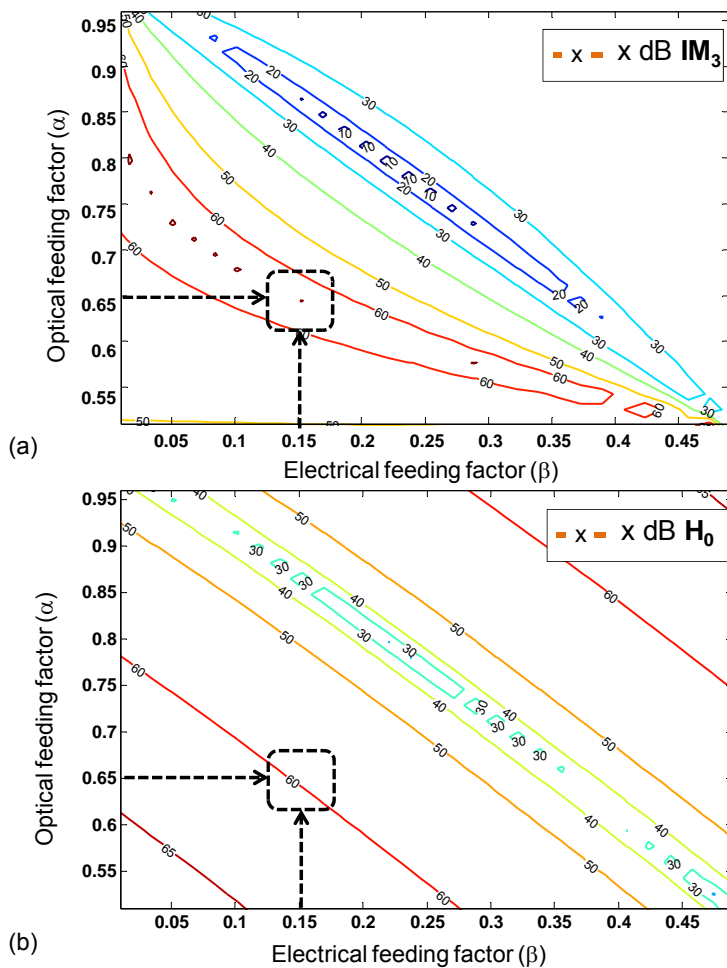

Figure 5. (a) IM_3 and (b) H_0 simulated values for a DPD-MZM scheme with 2 RF signals 1 GHz and 1.1 GHz and value region for IM_3 and H_0 according to selected electrical and optical feeding factors 0.65 and 0.15.

These ideal simulated results have been checked on a commercial Split-Step Fourier software simulation tool [9]. This simulation considers a dual parallel architecture with a MZM of 20 dB extinction ratio, 6 dB

of insertion losses and V_π near 1.5 V_{DC}. The simulation set-up comprises two ideal RF sources (ω_1 and ω_2) which allow us to evaluate IM$_3$ and HD$_3$. Optical attenuators and electrical delay lines are used to implement the RF and optical asymmetric feeding.

The α and β asymmetrical feeding factors have been properly selected in order to compare with the ideal feeding factors simulated previously.

These non-ideal simulation results, as shown in Table 1, agree with the behaviour of ideal simulation. For a 3 dB electrical attenuation (β = 0.25) and 18.5 dB optical attenuation (α = 0.49) values, a simulated 3rd harmonic distortion relation of 37.63 dB is obtained, which is slightly lower than ideal simulation results. These different results can be explained by taking into account insertion losses, bias voltage deviation and other sources of noise that have been considered by the optical network simulator tool, in this case VPItransmissionMaker.

Table 1. Simulation results for DPD-MZM configuration for non-ideal conditions

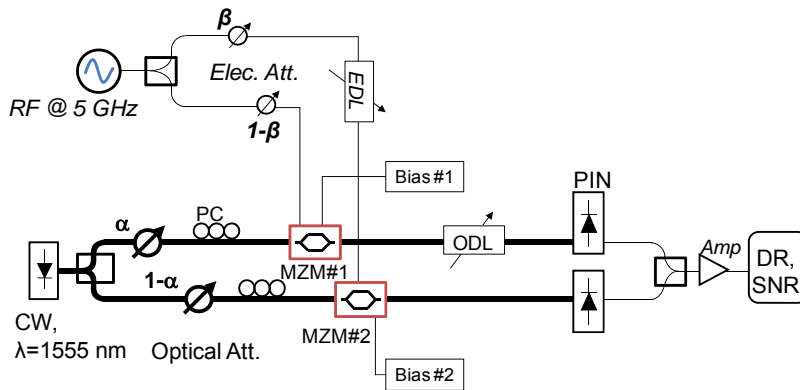| RF att. (β, dB)	Optical att. (α, dB)	HD$_3$ (dB)
3	18.5	37.63
4	20.5	39.60
5	21	41.66
6	25	43.67
7	26	45.60

Figure 6. DPD-MZM experimental set up used at laboratory.

In order to validate simulation results an experimental study has been carried out. Figure 3 shows the experimental set-up for the proposed DPD-MZM scheme. This set-up comprises two commercial MZM with a low V_π from 1.5 to 2 V_{DC} and 6 to 8 dB insertion losses, both are biased at QB point to minimize IM_2 [1, 5]. The polarization voltage Bias#1 and Bias#2 were provided in order to accomplish with the expected QB point for each MZM around 1.75 V_{DC}. Moreover, this set-up includes a 6 dBm CW laser source at 1555 nm and a single-tone RF source centred at 5 GHz with a maximum output optical power of 15 dBm. The asymmetric feeding is achieved by configuring different RF and optical attenuation levels. The range of the RF attenuation is fixed at a range between 2 and 6 dB, whereas the optical attenuation is between 0.5 to 22 dB. The electrical attenuation related to the asymmetrical feeding factor was fixed by a variable step RF attenuator and the optical attenuation was performed by a variable single mode inline fibre optical attenuator, as depicted in Figure 4. The used of an electrical delay line (EDL) and an optical delay line (ODL) of 330 ps has been considered in this experimental set-up in order to adjust and minimize the effect of the temporal drifts in the optical and RF electrical signals due to different lengths of the paths for each parallel MZM branch. Figure 4 shows HD_3 results for different experimental values of RF and optical attenuation. The 6 dB RF fixed attenuation simulation results are also included. It can be observed that the experimental DPD-MZM architecture obtains a HD_3 improvement close to 20 dB over HD_3 single MZM result that was 31.83 dB at HD_3, as depicted in Figure 4.
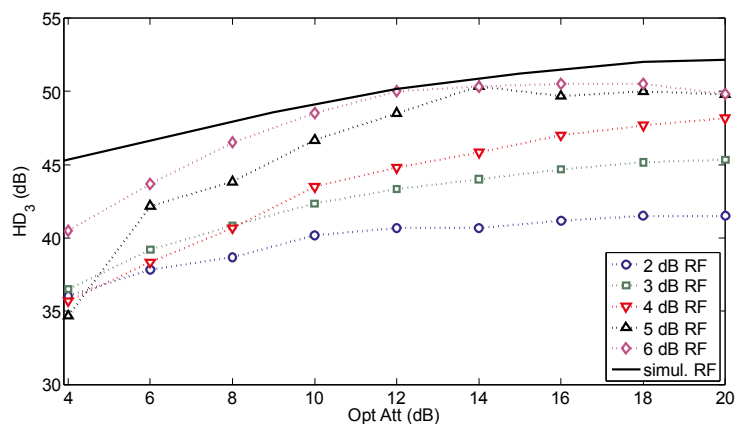

Figure 4. Experimental (dotted line) and simulated HD_3 results versus different optical attenuation values for a fixed RF attenuation.

Experimental results show that asymmetric feeding values should move between $\alpha = [0.66 - 0.95] \rightarrow [16 - 21]\,dB$ and $\beta = [0.05 - 0.20] \rightarrow [5 - 8]\,dB$ in order to maximize HD$_3$. These experimental asymmetric factors agree with the simulated results. Moreover, the PD-MZM performance can be enhanced carrying a balanced detection [12] and implementing a push-pull configuration on parallel MZM architectures to improve dynamic range [13].

Figure 5 shows experimental and simulation carrier power (H_0) results. The experimental values of H_0 are slightly higher than the simulated one due to an overestimation of the optical and electrical sources in the simulation tests. In this figure, H_0 decreases with asymmetric feeding factors that maximize HD$_3$. This constraint has to be considered in order to face the design of an integrated DPD-MZM architecture in one device.
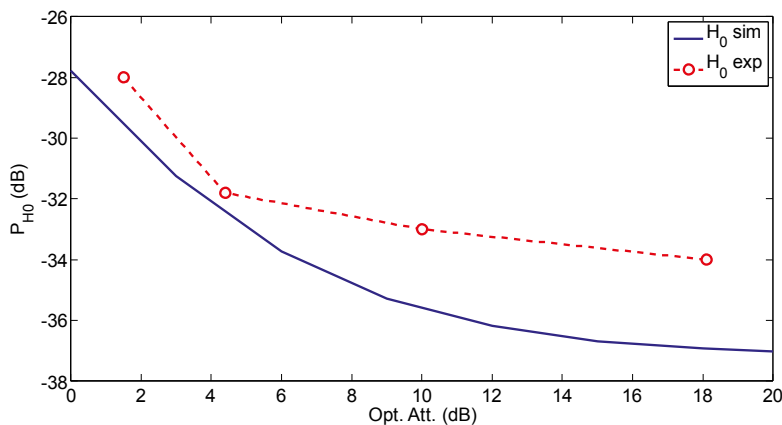

Figure 5. Simulation and experimental carrier power level H_0 with 6 dB fixed RF attenuation

The experimental results indicate that this technique improves the third harmonics rejection on a microwave carrier with improvements in the range of 15-20 dB compared with a single MZM. On the other hand it suppose a first step on the implementation of dual parallel linearization technique on a more robust design that includes components off-the-self. On the other hand, next steps will drive to an integration of this system on a one device dual-parallel MZM that will include all the considerations of differential photodetection and others in order to improve the behaviour of the linearization technique in broadband communications systems.

3.   Conclusions

The proposed dual configuration achieves a 20 dB HD$_3$ improvement over a single QB biased MZM modulator, when using properly designed RF and optical asymmetrical feeding factors. Simulated and experimental results show that this DPD-MZM architecture is an efficient broadband linear technique to improve MZM modulator performance. The results of the analytical and simulation evaluation demonstrated that this architecture is valid for broadband communications systems and the experimental set-up indicates the feasibility to implement this linearization technique with a microwave carrier of 5 GHz.

References

[1] C.H. Cox, Analog optical links: theory and practice, Cambridge University Press2004.
[2] H. Nagata, G.D. Feke, L. Yagang, W.R. Bosenberg, DC drift of Z-cut LiNbO3 modulators, Photonics Technology Letters, IEEE, 16 (2004) 1655-1657.
[3] S. Dubovitsky, W.H. Steier, S. Yegnanarayanan, B. Jalali, Analysis and improvement of Mach-Zehnder modulator linearity performance for chirped and tunable optical carriers, Lightwave Technology, Journal of, 20 (2002) 886-891.
[4] E.I. Ackerman, Broad-band linearization of a Mach-Zehnder electrooptic modulator, Microwave Theory and Techniques, IEEE Transactions on, 47 (1999) 2271-2279.
[5] A. Ferreira, T. Silveira, D. Fonseca, R. Ribeiro, P. Monteiro, External modulator linearization techniques for high performance radio over fiber transmission systems, Transparent Optical Networks, 2009. ICTON '09. 11th International Conference on, 2009, pp. 1-4.
[6] A.V. Cartaxo, T.M. Alves, Theoretical and experimental performance evaluation methods for DD-OFDM systems with optical amplification, Journal of Microwaves, Optoelectronics and Electromagnetic Applications, 10 (2011) 82-94.
[7] T.M. Alves, A.V. Cartaxo, Transmission of OFDM-UWB Radio Signals in IM–DD Optical Fiber Communication Systems Employing Optimized Dual Parallel Mach–Zehnder Modulators, Journal of Optical Communications and Networking, 5 (2013) 159-171.
[8] S. Li, X. Zheng, H. Zhang, B. Zhou, Highly linear radio-over-fiber system incorporating a single-drive dual-parallel Mach–Zehnder modulator, Photonics Technology Letters, IEEE, 22 (2010) 1775-1777.
[9] S.K. Korotky, R.M. de Ridder, Dual parallel modulation schemes for low-distortion analog optical transmission, Selected Areas in Communications, IEEE Journal on, 8 (1990) 1377-1381.
[10]C.H. Cox III; E. I. Ackerman, G. Betts, J.L. Prince, Limits on the performance of RF-over-fiber links and their impact on device design, Microwave Theory and Techniques, IEEE Transactions on , 54 (2006), 906-920.
[11] J.L. Corral, J. Marti, J.M. Fuster, General expressions for IM/DD dispersive analog optical links with external modulation or optical up-conversion in a Mach-Zehnder electrooptical modulator, Microwave Theory and Techniques, IEEE Transactions on, 49 (2001) 1968-1976.

[12] A. Joshi, X. Wang, D. Mohr, D. Becker, C. Wree, Balanced photoreceivers for analog and digital fiber optic communications, Defense and Security, International Society for Optics and Photonics 2005, pp. 39-50.
[13] S. Gupta, B. Jalali, 2nd order distortion cancellation in photonic time stretch analog-to-digital converter, Microwave Symposium, 2007. IEEE/MTT-S International, IEEE, 2007, pp. 229-232.